Am J Transl Res 2017;9(10):4640-4651
www.ajtr.org /ISSN:1943-8141/AJTR0057325

Original Article

Effects of targeted CD97 immune epitopes small interference RNA on cellular biological behaviors in MDA-MB231 malignant breast cancer cell line

Hua Tian*, Yang Chen*, Jian-Gang Zhao, Da-Ren Liu, Wei-Hua Gong, Li Chen, Yu-Lian Wu, Jian-An Wang

*Department of Surgery, 2nd Affiliated Hospital of Zhejiang University School of Medicine, Hangzhou 310009, Zhejiang Province, China. *Equal contributors.*

Received December 10, 2016; Accepted July 28, 2017; Epub October 15, 2017; Published October 30, 2017

Abstract: Two CD97 immune epitopes, $CD97^{EGF}$ (epidermal growth factor domain) and $CD97^{Stalk}$ (stalk domain), have different distribution patterns in malignant epidermal tumors. However, little is known about the effect of $CD97^{EGF}$ and $CD97^{Stalk}$ immune epitopes in breast cancer metastasis. To explore the effects on cell proliferation, infiltration, apoptosis, and the cell cycle, we used small interfering RNA (siRNA) against $CD97^{EGF}$ and $CD97^{Stalk}$ immune epitopes to knock down CD97 in MDA-MB231 breast cancer cells. Compared with controls, CD97 knockdown caused decreased cell growth, proliferation, migration, infiltration, and altered distribution of the percentage of cells in G0/G1 and S phase. We suggest that the potential mechanism of $CD97^{EGF}$ and $CD97^{Stalk}$ immune epitopes on the biological behaviors of MDA-MB231 breast cancer cells may be related to the altered number of N-terminal glycosylation sites, which influence the stability and signaling intensity of CD97 heterodimers.

Keywords: Immune epitopes, CD97, small interfering RNA (siRNA), breast cancer

Introduction

CD97 is a member of the seven-span transmembrane (TM7) subfamily of G-coupled protein receptors, with a molecular weight of 75 to 90 kDa [1]. The structure of CD97 consists of an extended extracellular region consisting of a signal peptide and several N-terminal epidermal growth factor (EGF) domains coupled to the TM7 domain by a conserved stalk region, and short intracellular segments at the C-terminus [2]. Importantly, CD97 is expressed in various types of epithelial carcinomas, and its expression levels correlate with the degree of dedifferentiation and tumor stage. CD97 interaction with its ligand, CD55, plays an important role in intracellular adhesion. CD97 is widely expressed on various normal cell types, including immune cells, epithelial cells, and hematopoietic stem and progenitor cells, and participates in invasive behaviors and metastasis of malignant epithelial tumor cells [4]. Increased CD97 expression also occurs in advanced colorectal, pancreatic, esophageal, and oral squamous cell carcinomas, where it predicts patient prognosis [7-10].

Wobus M *et al.* [5] showed that CD97 immune epitopes have differential accessibility to the CD97 monoclonal antibody, resulting in different staining patterns of the EGF domain ($CD97^{EGF}$) and the stalk region ($CD97^{Stalk}$). Importantly, the role of the $CD97^{EGF}$ and $CD97^{Stalk}$ immune epitopes on the cellular signaling competency of malignant cells has not been intensively studied [4, 6, 7]. CD97 immune epitopes are not homogenously present on normal and malignant cells and tissues, and therefore, the use of monoclonal antibodies results in different staining patterns of $CD97^{EGF}$ and $CD97^{Stalk}$ [5]. For example, $CD97^{EGF}$ and $CD97^{Stalk}$, have different distribution patterns in malignant epidermal tumor tissue and gastrointestinal smooth muscle cells [5, 11]. Additionally, we previously demonstrated that $CD97^{EGF}$ and $CD97^{Stalk}$ immune epitopes have different staining patterns in malignant breast cancer (data has not been published) and gastric cancer patient tissues [11, 14].

Cell type-specific N-glycosylation also affects antibody accessibility to CD97 immune epitopes. Moreover, N-glycosylation not only affects the accessibility of $CD97^{EGF}$ and $CD97^{Stalk}$ epitopes on malignant cells in solid and nonsolid tumor tissues, but also alters CD97 binding to CD55 [12, 13]. How $CD97^{EGF}$ and $CD97^{Stalk}$ interactions with CD55 influence downstream signal transduction in tumor cells remains unclear. Recently, CD97 was identified as an adhesion GPCR that affects lysophosphatidic 1 (LPA1) in MDA-MB-231 breast cancer cells; transfection of CD97 small interfering RNA (siRNA) blocked the LPA-induced increase in intracellular Ca^{2+}, indicating that CD97 plays a role in LPA1-CD97/Gi/o proteins/phospholipase C/IP3/Ca^{2+} signaling in breast cancer cells [15]. However, little is known about the effect of $CD97^{EGF}$ and $CD97^{Stalk}$ immune epitopes in breast cancer metastasis. In the present study, we designed and constructed siRNAs targeting CD97 immune epitopes, and transfected them into breast cancer cell lines to investigate the individual roles of $CD97^{EGF}$ and $CD97^{Stalk}$ immune epitopes in the biological behavior of breast cancer cells, focusing on cell growth, proliferation, and migration.

Materials and methods

Cell lines

Human malignant breast cancer lines MDA-MB231, MDA-468, MCF-7, and T47D were purchased from the Oncology Institute of ZheJiang University School of Medicine.

Antibodies and reagents

We utilized the following antibodies: horseradish peroxidase tagged sheep rabbit IgG from Cell Signaling Technology (Beverly, MA, USA), anti-CD97 polyclonal antibody from Abnova Biotechnology Corporation (Walnut, CA, USA), anti-$CD97^{EGF}$ monoclonal antibody (VIM-3b), anti-$CD97^{Stalk}$ monoclonal antibody (MEM-180) from Abcam (Cambridge, MA, USA), and anti-β-actin from Sigma (St. Louis, MO, USA). DMEM culture media and fetal calf serum were purchased from HyClone Corporation (Logan, Utah, USA). Protein extraction was from PIERCE Biotechnology Corporation (Rockford, Illinois, USA). Protein liquid chromogenic agent was from Santa Cruz Biotechnology (CA, USA). SiRNAnboFECT™CP transfection regents were purchased from Ruibo Biotechnology (Guangzhou, China). The MTT cell proliferation and cytotoxicity detection kit was from BiYunTian (ShangHaim, China). The TUNEL apoptosis detection kit was from PROMEGA Biotechnology Corporation (Madison, Wisconsin, USA) and the Transwell Cell Migration Kit was from Corning incorporation (Corning, NY, USA).

Cell culture

Human MDA-MB231, MDA-468, MCF-7, and T47D breast cancer cell lines were cultured in DMEM, containing 10% fetal calf serum, 100 u/ML penicillin, and 100 u/ML streptomycin, and maintained at 37°C in a 5% CO_2-saturated humidified incubator. Cells were passaged every seven days when they reached 70%~80% confluency using trypsin-EDTA, then transferred to serum-free medium for further experiment.

Western blotting

Total protein was extracted from cells using the RIPA lysis protein extraction kit (Pierce Biotechnology Corporation, Rockford, Illinois, USA). Equal amounts of protein were separated using 10% sodium dodecyl sulfate polyacrylamide gel electrophoresis (SDS-PAGE) and transferred to PVDF membranes (Hercules, CA, USA). After blocking with 5% non-fat milk for two hours, the membranes were incubated overnight at 4°C with polyclonal antibodies against CD97 (1:400) and β-actin (1:1000). Horseradish peroxidase tagged goat anti-rabbit IgG secondary antibody (1:5000) was applied for one hour at room temperature. The immunereactive protein bands were identified using an enhanced chemiluminescent kit. Signal intensity was measured using a BioRad XRS chemiluminescence detection system (BioRad Laboratories). The cell lines that expressed the highest levels of CD97 were used for experiments.

SiRNA design and screening

siRNAtargeting sequences for the $CD97^{EGF}$ and $CD97^{Stalk}$ immune epitopes were designed using the CD97 gene sequence (1-3353 bp) (Gene Bank NM_001025160.2) by smart siCatch™ siRNA design software. The targeting siRNAs for $CD97^{EGF}$ and $CD97^{Stalk}$ are located from 440 bp to 1120 bp, and 1150 bp to 1750 bp, respectively. Three pairs of siRNA for each CD97 immune epitope (siRNA$CD97^{EGF}$1-3 and siRNA$CD97^{Stalk}$1-3) were designed and optimized using mass spectrometry. siP069694-

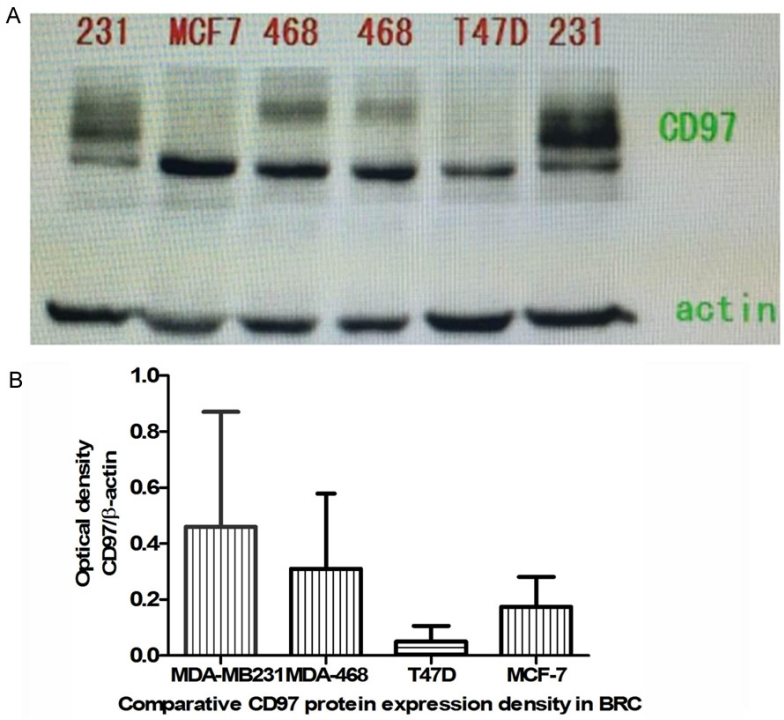

Figure 1. CD97 protein expression in breast cancer cell lines. A. CD97 protein expression in MDA-MB231, T47D, MCF-7, and MDA-468 human breast cancer cell lines was detected by western blotting. B. Quantification of western blots CD97 protein expression in malignant breast cancer cell lines.

73939 and siN05815122147 were selected as a GAPDH positive control (hGAPDH group) and negative control (Ncontrol group), respectively. After cells were cultured for one day, we transfected the siRNAs by using SiRNAnboFECT™CP transfection regents according to the manufacturer's instructions, and cultured cells for another 72 hours. The most efficiently targeted cells were screened by western blotting using antibodies against $CD97^{EGF}$ (VIM-3b, 1:200) and $CD97^{Stalk}$ (1:400).

Cell counting

$CD97^{EGF}$siRNA- and $CD97^{Stalk}$siRNA-transfected breast cancer cell lines were cultured in 24 well plates; four wells per condition were trypsinized every 24 hours and a single cell suspension was prepared for counting. Cell number was calculated using a hemacytometer as follows: cell number/ml = total number of four corner area $\times 10^4/4$. Experiments were performed in triplicate.

Cell proliferation assay

Cells transfected with NcontrolsiRNA, hGAPDHsiRNA, $CD97^{EGF}$siRNA, and $CD97^{Stalk}$siRNA were cultured at room temperature. Cell proliferation was measured using a MTT assay. A microplatespectrophotometer was used to read the MTT plate results at 490 nm.

Wound healing assay

SiRNA-transfected cells were plated at a density of 5×10^5 in six well plates and cultured for 24 hours. A pipet tip was scraped across the bottom of the dish and cells were then cultured in serum-free DMEM. The scar margin was analyzed at 12, 24, and 48 hours to evaluate the migration of each cell line.

Transwell infiltration assay

We plated cells on Transwell filter membranes (8 μM pores) (Corning Incorporated), and RPMI 1640 media supplemented with 20% fetal calf serum was added for one hour at room temperature. A nearly exactly equal number transfected $CD97^{EGF}$siRNA- and $CD97^{Stalk}$siRNA-expressing MDA-MB231 cells were added in the Transwell chamber, hGAPDHsiRNA positive group and N control siRNAnegtive group were performed as similar process. Cells were incubated at 37°C with 5% CO_2 for 48 hours. After washing the membranes, cells were fixed with 4% formalin and stained with crystal violet. Samples were analyzed using an inverted phase contrast microscope.

Apoptosis analysis

MDA-MB231 cells transfected with NcontrolsiRNA, hGAPDHsiRNA, $CD97^{EGF}$siRNA, or $CD97^{Stalk}$siRNA were cultured for 48 hours, then trypsinized and centrifuged. Apoptosis was determined using the TUNEL apoptosis detection kit according to the manufacturer's instructions.

Cell cycle analysis

Cells were trypsinized and centrifuged. Following a wash with phosphate-buffered saline,

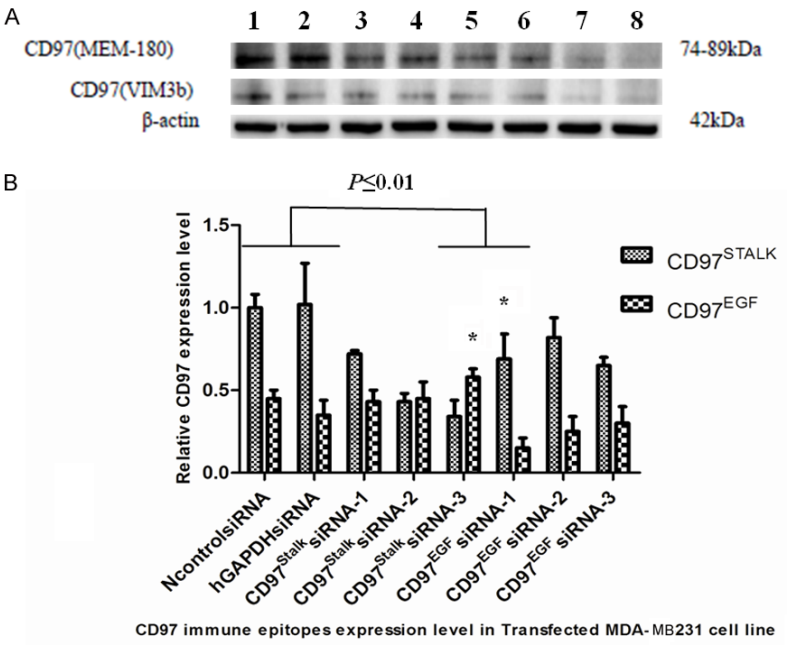

Figure 2. Generation of sensitive targeting siRNAs for $CD97^{EGF}$ and $CD97^{Stalk}$ immune epitopes. (A) Western blot for CD97 protein expression in: 1. NcontrolsiRNA group; 2. hGAPDHsiRNA group; 3. $CD97^{EGF}$siRNA-1 group; 4. $CD97^{EGF}$siRNA-2 group; 5. $CD97^{EGF}$siRNA-3 group; 6. $CD97^{Stalk}$siRNA-1 group; 7. $CD97^{Stalk}$siRNA-2 group; and 8. $CD97^{Stalk}$siRNA-3 group. (B) Quantification of western blots in (A). * indicates $P \leq 0.01$).

cells were fixed with 0.75 ml pure ethyl alcohol overnight. Next, cells were centrifuged at room temperature, and mixed with the DNA staining solution. After incubating for 30 minutes, the cell cycle of each group was detected by flow cytometry according to the cell cycle detection kit illustration.

Statistical analysis

Each experiment was performed in triplicate and the data is presented as mean ± SD. A *P* value of 0.05 or less was considered statistically significant. An one-way analysis of variance was used to compare samples. A *t*-test was applied to compare paired samples and a correlation test was analyzed using Spearman methods. *GraphPad Prism5.0* software was used for all statistical analyses and data management.

Results

Comparison of CD97 protein expression in breast cancer cell lines

The morphologies of the breast cancer cell lines we used in this study (MDA-MB231, MDA-468, MCF-7, and T47D) are shown in **Figure 1**. CD97 protein expression was detected in all four lines and is quantified in **Figure 1**, and MDA-MB231 cells were utilized for all following experiments for its highest CD97 protein expression and relative discrimination of CD97 immune epitopes expression.

CD97 knockdown efficiency and screening of siRNAs

Expression of $CD97^{EGF}$ and $CD97^{Stalk}$ immune epitopes was analyzed in MDA-MB-231 cells using western blotting analysis with domain-specific antibodies (**Figure 2**). We then tested the efficiency of the siRNAs targeting each domain. Compared to the control siRNA, the relative intensities ratio of the $CD97^{EGF}$ band following $CD97^{EGF}$siRNA transfection (siRNAs 1-3) were 0.25, 0.42, and 0.48 (**Figure 2**). The relative intensities ratio of $CD97^{Stalk}$ upon $CD97^{Stalk}$siRNA (1-3) transfection were 0.71, 0.43, and 0.34 (**Figure 2**). Therefore, we selected $CD97^{EGF}$siRNA-1 and $CD97^{Stalk}$siRNA-3 for all subsequent experiments.

Cell proliferation of CD97-deficient MDA-MB231 breast cancer cells

We measured the growth rate of MDA-MB231 cells transfected with $CD97^{EGF}$siRNA and $CD97^{Stalk}$siRNA by quantifying cell number over seven days. We found that both $CD97^{EGF}$ and $CD97^{Stalk}$ knockdown reduced cell growth compared to control siRNAs, although $CD97^{Stalk}$ knockdown had the stronger effect ($P<0.05$) (**Table 1**; **Figure 3**). Together, these results suggest that CD97 protein and its immune epitopes is important for controlling MDA-MB231 cell growth behaviors.

We measured the effect of CD97 knockdown on cell proliferation a second way using a MTT assay at 12, 24, and 48 hours. Similar to our previous result, we found that $CD97^{EGF}$siRNA- and $CD97^{Stalk}$siRNA-transfected MDA-MB231

Table 1. Effect of targeted CD97 knockdown on MDA-MB231 breast cancer cell growth

Transfected Groups	Cell number (×10^4)			
	Day 1	Day 3	Day 5	Day 7
CD97^{EGF}siRNA group	19.00	45.25	172.50	250.50
CD97^{Stalk}siRNA group	20.25	28.50*	85.25*	98.50$^{\#}$
NcontrolsiRNA group	20.25	120.25	265.25	459.25
hGAPDHsiRNA group	19.25	110.50	290.45	487.50

CD97^{Stalk}siRNA group compared with the CD97^{EGF}siRNA group (*P<0.05; $^{\#}P$<0.01).

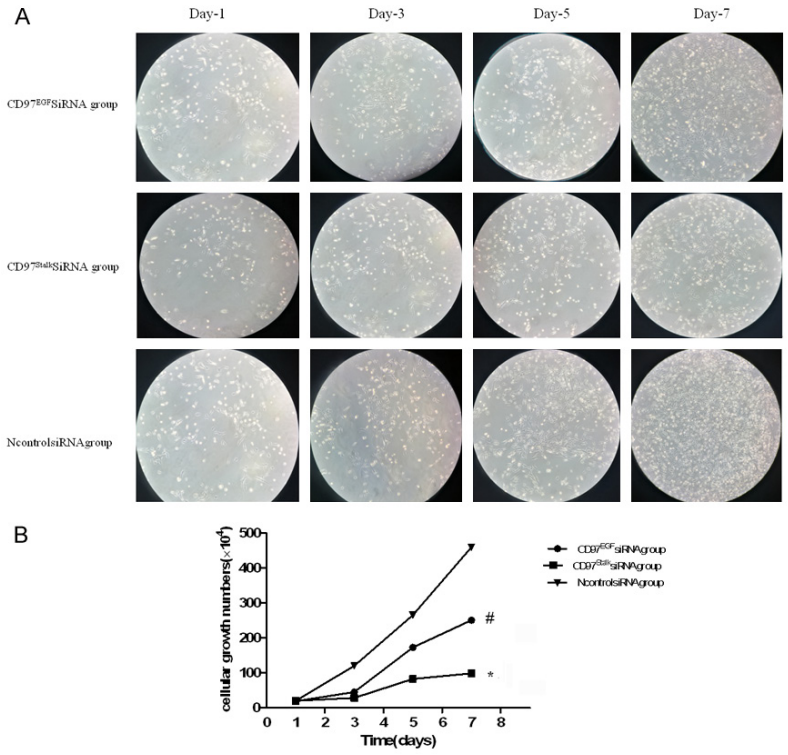

Figure 3. Effect of targeted CD97 siRNA transfection on human breast cancer cell growth. MDA-MB231 cells were transfected with CD97^{EGF}siRNA-1, CD97^{Stalk}-siRNA-3, negative control siRNA, or hGAPDHsiRNA, and cultured for seven days. Cells were counted on day 3, day 5, and day 7. A. Microscopic images of transfected MDA-MB231 malignant breast cancer cells on day 1, day 3, day 5, and day 7. B. Comparison of cell number of differentially transfected MDA-MB231 cells over seven days ($^{\#}P$<0.05; *P<0.01).

cells had significantly lower proliferation than the NcontrolsiRNA group and the hGAPDHsiRNA group (P<0.05) (**Figure 4A**). Additionally, the inhibitory effect on cell proliferation by CD97^{Stalk} knockdown was significantly lower than CD97^{EGF} knockdown (P<0.05) (**Table 2**; **Figure 4B**).

Effect of CD97 knockdown on migration of MDA-MB231 cells

The migration of CD97^{EGF}siRNA- and CD97^{Stalk}-siRNA-transfected cells was quantified following a wound healing assay after 12, 24, and 48 hours. We found that both CD97^{EGF} and CD97^{Stalk} knockdown reduced cell migration compared to the NcontrolsiRNA and hGAPDHsiRNA groups (P<0.01) (**Figure 4C**). Additionally, the distance covered by CD97^{Stalk}-siRNA-transfected MDA-MB231 cells was significantly lower than that of CD97^{EGF}siRNA-transfected cells (P<0.05) (**Table 3**; **Figure 4D**).

Transwell infiltration competence of CD97-deficient MDA-MB231 cells

We measured the ability of CD97-deficient MDA-MB231 cells to infiltrate the gel membrane of Transwell chambers. The number of infiltrating cells in the CD97^{EGF}siRNA group, CD97^{Stalk}siRNA group, NcontrolsiRNA group, and hGAPDHsiRNA group after 48 hours were 75.5±5.0, 48.6±3.5, 180±11.0, and 209±5.0 (×10^3), respectively. The number of infiltrating CD97^{Stalk}siRNA cells was significantly less than in the other three groups (P<0.05). Therefore, our results indicate that the inhibitory effects of CD97^{Stalk} knockdown on MDA-MB231 cell migration are more efficient than CD97^{EGF} knockdown (**Figure 4E**, **4F**).

Apoptosis of CD97siRNA-transfected MDA-MB231 cells

The apoptosis rates of the CD97^{EGF}siRNA group, CD97^{Stalk}siRNA group, NcontrolsiRNA group, and hGAPDHsiRNA group after 48 hours were 2.67%, 2.90%, 3.37%, and 3.4%, respectively. The flow cytometry results indicate that target-

A

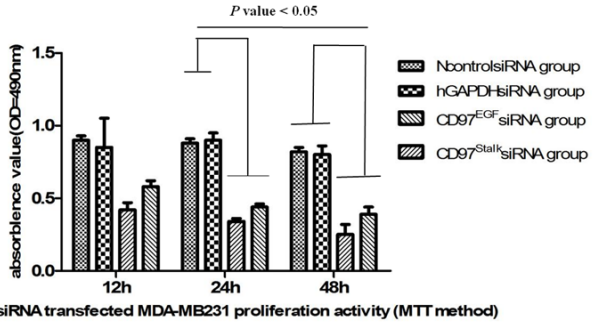

CD97siRNA transfected MDA-MB231 proliferation activity (MTT method)

B

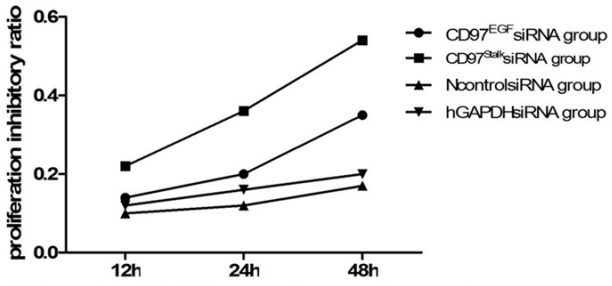

CD97siRNA transfected MDA-MB231 proliferation inhibitory ratio curve

C

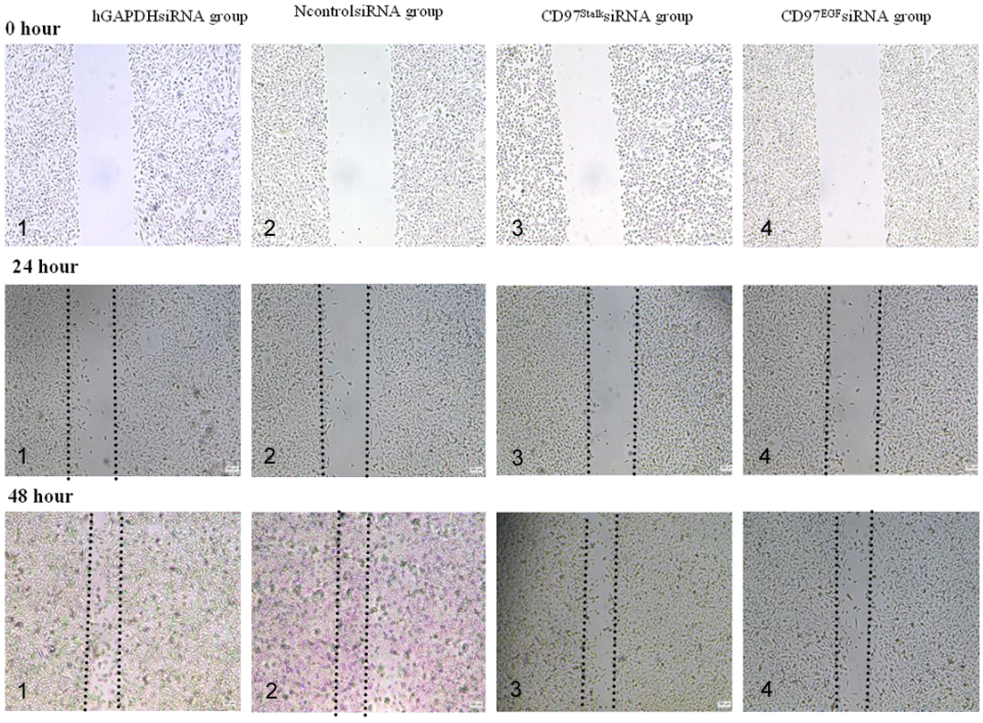

D

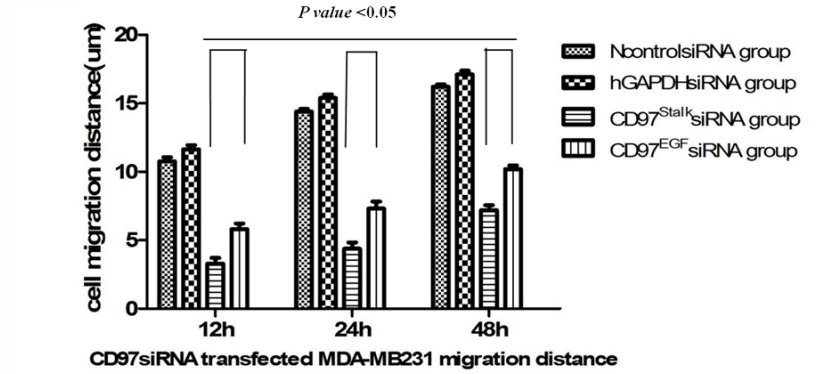

CD97siRNA transfected MDA-MB231 migration distance

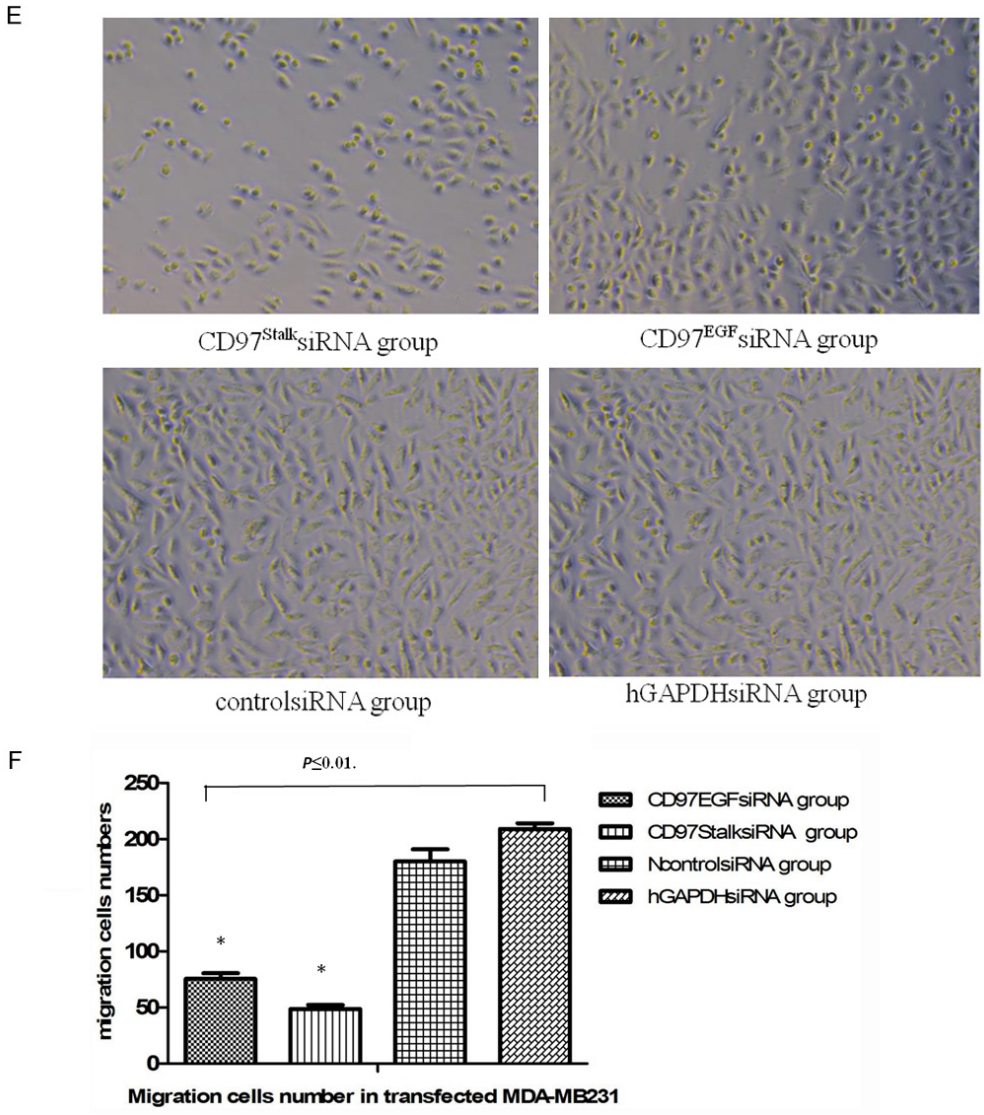

Figure 4. Effects of targeted CD97 knockdown on proliferation, migration, and invasion of MDA-MB231 breast cancer cells. (A) Rate of proliferation of transfected MDA-MB231 breast cancer cells using a MTT assay. (B) Proliferation inhibitory ratio curve of transfected MDA-MB231 breast cancer cells ($P<0.05$). Microscopic images (C) and bar graph (D) illustrating the results of the wound healing assay ($P<0.01$). (E) Microscopic images of infiltrating MDA-MB231 cells in the Transwell infiltration assay. (F) Bar graph showing the number of infiltrating cells ($\times 10^4$) in (E) ($P<0.05$).

ed CD97 knockdown has negligible effects on MDA-MB231 cell apoptosis (**Figure 5A**, **5B**).

Cell cycle analysis of CD97siRNA-transfected MDA-MB231 cells

The number of cells in G0/G1, S, and G2/M stages in $CD97^{EGF}$siRNA and $CD97^{Stalk}$siRNA groups were significantly different compared to the NcontrolsiRNA and hGAPDHsiRNA groups. The distribution of cells in G0/G1 in CD97siRNA groups was decreased, while the number of cells in S stage was increased ($P<0.05$) (**Figure 5C**; **Table 4**). Similar to our previous results, we found that the effect on cell cycle was more pronounced in the $CD97^{Stalk}$siRNA group compared to the $CD97^{EGF}$siRNA group. Our results indicate that CD97 knockdown retards MDA-MB231 cell proliferation (**Figure 5D**) and suggest the $CD97^{EGF}$ and $CD97^{Stalk}$ immune epitopes decrease the rate of MDA-MB231 cell proliferation while G0/G1 phase cell cycle were arrested.

Table 2. Proliferation of targeted CD97 siRNA-transfected MDA-MB231 cells

Transfected Groups	12 h		24 h		48 h	
	OD_{490}	IR	OD_{490}	IR	OD_{490}	IR
$CD97^{EGF}$siRNA group	0.58±0.04	0.14	0.44±0.02	0.20	0.39±0.05	0.35
$CD97^{Stalk}$siRNA group	0.42±0.05	0.22	0.34±0.02	0.36*	0.25±0.07	0.54*
NcontrolsiRNA group	0.90±0.03	0.10	0.88±0.03	0.12	0.82±0.03	0.17
hGAPDHsiRNA group	0.85±0.12	0.12	0.90±0.05	0.16	0.80±0.06	0.20

*$CD97^{Stalk}$siRNA group compared with $CD97^{EGF}$siRNA group (P<0.01).

Table 3. Migration distance of transfected MDA-MB231 breast cancer cell lines (μm)

Transfected Groups	12 h	24 h	48 h
$CD97^{EGF}$siRNA group	3.30±0.40*	4.37±0.48*	7.20±0.36*
$CD97^{Stalk}$siRNA group	5.80±0.43#	7.31±0.52#	10.20±0.26#
NcontrolsiRNA group	10.75±0.30	14.40±0.20	16.20±0.18
hGAPDHsiRNA group	11.65±0.30	15.40±0.24	17.10±0.28

$CD97^{Stalk}$siRNA group (*) compared with $CD97^{EGF}$siRNA group (#) (P<0.05).

Discussion

Dysregulation of cell growth and proliferation contributes to the induction of tumorigenesis [16, 17]. CD97 is a member of the seven-span transmembrane (TM7) receptor subfamily and is also referred to as EGF-TM7 [1]. EGF-TM7 family members form heterodimers through their repeated EGF domains and binding of different ligands results in specific signaling pathway initiation within the cell. Interaction between CD97 and its ligands (CD55, integrin α5ß1, and chondroitin sulfate) contributes to tumorigenesis through cell adhesion, migration, and angiogenesis through G-protein-dependent or G-protein-independent signaling [12].

Protein shearing at the eight N-terminal glycosylation sites on the extracellular domain of CD97 alters its molecular weight [5] and the different number of N-terminal glycosylation sites on the $CD97^{EGF}$ and $CD97^{Stalk}$ immune epitopes regulates CD97 tumor cell signaling [20]. In particular, the affinity of $CD97^{EGF}$ immune epitopes for the monoclonal antibody depends on N-terminal glycosylation. In vitro experiments have demonstrated that inhibitory glycosylation and glycosylation action site mutation of the $CD97^{EGF}$ domain is required and impacted the affinity of $CD97^{EGF}$ monoclonal antibody and its ligand CD55 combination [5]. A mutation in the N-terminal glycosylation site, or lack of glycosylation can interfere with the immune response and binding competence of $CD97^{Stalk}$ and $CD97^{EGF}$ immune epitopes to the monoclonal antibody. For CD97 EGF domain has three glycosylation sites in the N-terminus and five glycosylation sites in the stalk region, but the regulation mechanisms of glycosylation and its interaction between EGF domain and stalk region still have not been clarified. The first two sites in the EGF domain have a more significant effect on monoclonal antibody binding compared with the third glycosylation site in the second CD97 EGF domain [5]. Expression of $CD97^{EGF}$ and $CD97^{Stalk}$ immune epitopes can be detected on solid epithelial tumors, and have different staining patterns tested by using opposite monoclonal antibodies [5]. Compared with the lower expression of $CD97^{EGF}$ immune epitopes, $CD97^{Stalk}$ expression is more commonly found in metastatic digestive tract epithelial carcinoma cells [7, 11]. $CD97^{Stalk}$ immune epitopes are highly expressed in the smooth muscle cells of the gastrointestinal tract, and higher expression of $CD97^{Stalk}$ immune epitopes on smooth muscle cells indicates which is responsible for the motile and contractile competence compared to tumor cells that metastasize [5].

CD97 is a typical G-protein coupled receptor that is involved in cell proliferation, differentiation, and apoptosis [21]. CD97 has a unique structure, composed of an extracellular α subunit and a seven-pass transmembrane β subunit, which mediates its role in cellular processes [1]. The formation of CD97 heterodimers is the initiating step of signal transduction, and the β subunit is involved in promoting the formation of homo- and heterodimers. CD97 heterodimers activate the RHO signaling pathway by binding the LPA receptor (LPA1-CD97/Gi/o protein/phospholipase C/IP3/Ca^{2+}), which interacts with intracellular Gα12/13 protein, lead-

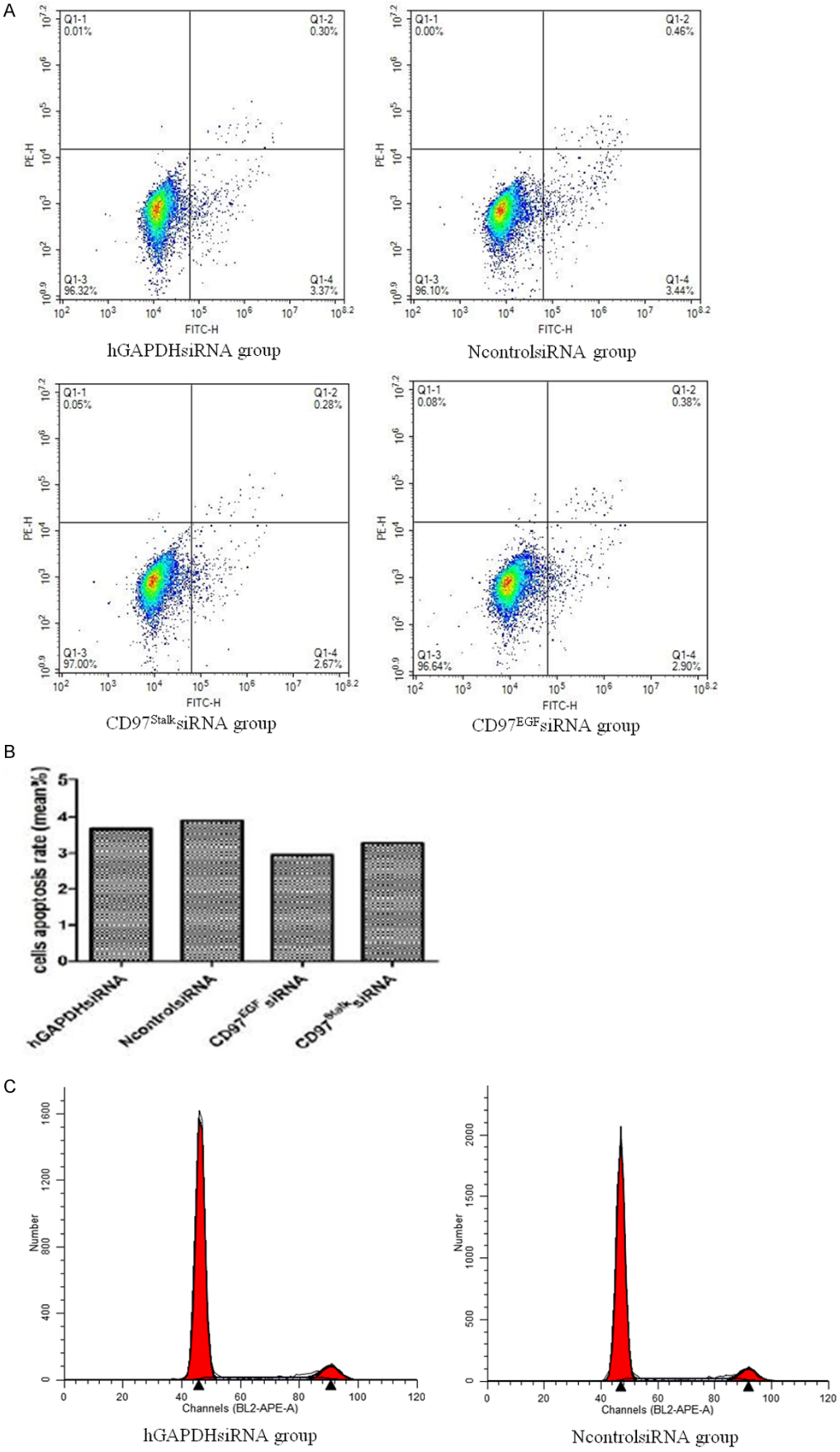
A
Q1-1 0.01%
Q1-2 0.30%
Q1-3 96.32%
Q1-4 3.37%
PE-H
FITC-H
hGAPDHsiRNA group
Q1-1 0.00%
Q1-2 0.46%
Q1-3 96.10%
Q1-4 3.44%
NcontrolsiRNA group
Q1-1 0.05%
Q1-2 0.28%
Q1-3 97.00%
Q1-4 2.67%
CD97StalksiRNA group
Q1-1 0.08%
Q1-2 0.38%
Q1-3 96.64%
Q1-4 2.90%
CD97EGFsiRNA group
B
cells apoptosis rate (mean%)
hGAPDHsiRNA
NcontrolsiRNA
CD97EGF siRNA
CD97Stalk siRNA
C
Number
Channels (BL2-APE-A)
hGAPDHsiRNA group
NcontrolsiRNA group

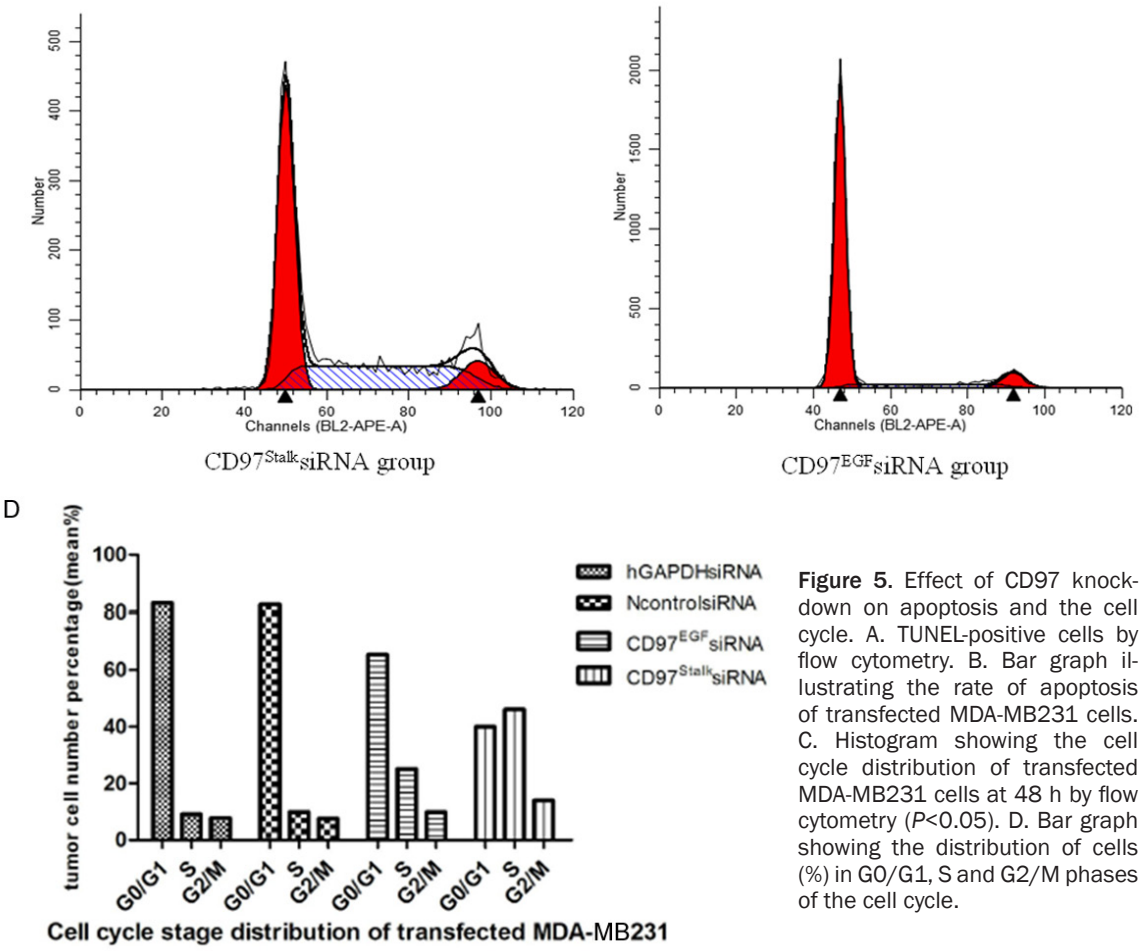

Figure 5. Effect of CD97 knockdown on apoptosis and the cell cycle. A. TUNEL-positive cells by flow cytometry. B. Bar graph illustrating the rate of apoptosis of transfected MDA-MB231 cells. C. Histogram showing the cell cycle distribution of transfected MDA-MB231 cells at 48 h by flow cytometry (P<0.05). D. Bar graph showing the distribution of cells (%) in G0/G1, S and G2/M phases of the cell cycle.

Table 4. Cell cycle distribution of siRNA-treated MDA-MB231 breast cancer cells

Transfected groups	Cells (mean %)		
	G0/G1	S	G2/M
hGAPDHsiRNA group	83.01%	9.13%	7.86%
NcontrolsiRNA group	82.54%	9.84%	7.61%
$CD97^{EGF}$siRNA group	65.39%	25.08%	9.53%
$CD97^{Stalk}$siRNA group	39.92%	46.15%	13.93%

ing to increased RHO-GTP levels and activation of the Rho kinase α [22]. Intracellular Rho kinase α stimulates Src and fos promoter transcription through MAPK signaling. And the glycosylation regulation sites of EGF domain and Stalk region of CD97 protein maybe participated the CD97 heterodimers formulation and even inducing tumor-promoting morphological changes, such as cellular matrix adhesion and cytoskeletal reconstruction [5].

RNA interference (RNAi) technology is an efficient genetic tool to replace gene knockout methods. Its benefits include high efficiency and high selectivity for elimination of targeted gene expression. RNAi is widely used as a tool for determining gene function in malignant cell behavior through downregulation or inhibition of targeted gene expression (gene silencing effect) [23]. To explore the function of $CD97^{EGF}$ and $CD97^{Stalk}$ immune epitopes in breast cancer, $CD97^{EGF}$ and $CD97^{Stalk}$ immune epitopes were targeted with siRNA. CD97 knockdown resulted in decreased cell growth and proliferation, as well as motility and infiltrative phenotypes. Targeted CD97 immune epitope knockdown prolonged the cell cycle in MDA-MB231 cells, and also altered its distribution of different cell stages in the cell cycle. Compared with $CD97^{EGF}$ knockdown, $CD97^{Stalk}$ knockdown had a significant inhibitory effect on the above cellular behaviors. Our study suggests that CD97 is a versatile multifunctional protein which participates in proliferation, migration, and infiltration.

$CD97^{EGF}$ and $CD97^{Stalk}$ immune epitopes have multiple glycosylation sites at the N-terminus, a

region of pivotal proteolysis [25]. Targeted siRNA knockdown inhibits CD97 immune epitope expression and alters the number of N-terminal glycosylation sites, which may influence the stability and signaling capabilities of CD97 heterodimers. As a result, CD97 immune epitope knockdown changed the cellular biological behaviors. The greater number of N-terminal glycosylation sites in the $CD97^{Stalk}$ domain may partly account for the stronger inhibitory effects of its knockdown compared to the $CD97^{EGF}$ domain. From the structure of CD97 protein and its immune epitopes glycosylation sites distribution characteristics, we find the inhibitory effects of targeted small interfere RNA on the CD97 immune epitopes expression, and N-terminal glycosylation sites number changes also leads to the cellular signal transduction intensity and stability of CD97 heterodimer formation. Furthermore, there may be exists an ascending effects from the initiated glycosylation sites to the terminal glycosylation site, so this speculation need to be deep demonstrated by structural biological method in future. Together, our observations show that targeted $CD97^{EGF}$ and $CD97^{Stalk}$ immune epitope knockdown in MDA-MB231 breast cancer cells lines affects cell proliferation, migration, infiltration, and cell cycle. Our studies demonstrated that CD97 immune epitopes play an important role on breast cancer cell lines cellular biological behaviors even in cell signal transduction pathway.

Acknowledgements

This work was supported by a grant from the Nature Science Fund of Zhejiang Province (Grant No. LY16H030007).

Disclosure of conflict of interest

None.

Address correspondence to: Li Chen, Department of General Surgery, 2nd Affiliated Hospital of Zhejiang University School of Medicine, Hangzhou 310009, Zhejiang Province, China. Tel: +086-137-3818-7296; E-mail: chenli_hzxs@sina.com

References

[1] Gordon S, Hamann J, Lin HH, Stacey M. F4/80 and the related adhension-GPCRs. Eur J Immunol 2011; 41: 2472-2776.

[2] Pierce K, Premont RT, Lefkowitz RJ. Seven-transmembrane receptors. Nat Rev Mol Cell Biol 2002; 3: 639-650.

[3] Capasso M, Durrant LG, Stacey M, Gordon S, Ramage J, Spendlove I. Costimulation via CD55 on human CD4+ T cells mediated by CD97. J Immunol 2006; 177: 1070-1077.

[4] Eichler W, Hamann J, Aust G. Expression characteristics of the human CD97 antigen. Tissue Antigens 1997; 50: 429-438.

[5] Wobus M, Vogel B, Schmücking E, Hamann J, Aust G. N-Glycosylation of CD97 within the EGF domains is crucial for epitope accessibility in normal and malignant cells as well as CD55 ligand binding. Int J Cancer 2004; 112: 815-822.

[6] Eichler W. CD97 isoform expression in leukocytes. J Leukoc Biol 2000; 68: 56l-567.

[7] Han SL, Xu C, Wu XL, Li JL, Liu Z, Zeng QQ. The impact of expressions of CD97 and its ligand CD55 at the invasion front on prognosis of rectal adenocarcinoma. Int J Colorectal Dis 2010; 25: 695-702.

[8] HOANG-VU C, Bull K, Schwarz I, Krause G, Schmutzler C, Aust G, Köhrle J, Dralle H. Regulation of CD97 protein in thyroid carcinoma. J Clinl Endocrinol Metab 1999; 84: 1104-1109.

[9] Liu D, Trojanowicz B, Radestock Y, Fu T, Hammje K, Chen L, Hoang-Vu C. Role of CD97 isoforms in gastric carcinoma. Int J Oncol 2010; 36: 1401-1408.

[10] Aust G, Steinert M, Schlitz, Boltze C, Wahlbuhl M, Hamann J, Wobus M. CD97, but not its closely related EGF-TM7 family member EMR2, is expressed on gastric, pancreatic, and esophageal carcinomas. Am J Clin Pathol 2002; 118: 699-707.

[11] Liu Y, Chen L, Hoang-Vu C, Chen Z, Gimm O, Finke R, Hoang-Vu C. The expression of $CD97^{EGF}$ and its ligand CD55 on marginal epithelium is related to higher stage and depth of tumor invasion of gastric carcinomas. Oncol Rep 2005; 14: 1413-1420.

[12] Safaee M, Clark AJ, Ivan M, Oh MC, Bloch O, Sun MZ, Oh T, Parsa AT. CD97 is a multifunctional leukocyte receptor with distinct role in human cancers (review). Int J Oncol 2013; 43: 1343-1350.

[13] Abbott RJ, Spendlove I, Roversi P, Fitzgibbon H, Knott V, Teriete P, McDonnell JM, Handford PA, Lea SM. Structural and functional characterization of a novel T cell receptor Co-regulatory protein complex, CD97-CD55. J Biol Chem 2007; 282: 22023-22032.

[14] Liu D, Li C, Trojanowicz B, Li X, Shi D, Zhan C, Wang Z, Chen L. CD97 promotion of gastric carcinoma lymphatic metastasis is exosome

dependent. Gastric Cancer 2016; 19: 754-766.
[15] Park SJ, Lee KP, Kang S, Chung HY, Bae YS, Okajima F, Im DS. Lysophosphatidylethanolamine utilizes LPA(1) and CD97 in MDA-MB-231 breast cancer cells. Cell Signal 2013; 25: 2147-2154.
[16] Zhang J, Yao H, Song G, Liao X, Xian Y, Li W. Regulation of epithelial-mesenchymal transition by tumor-associated macrophages in cancer. Am J Transl Res 2015; 7: 1699-1711.
[17] Hanahan D, Weinberg RA. Hallmarks of cancer: the next generation. Cell 2011; 144: 646-674.
[18] Guido C, Whitaker-Menezes D, Capparelli C, Balliet R, Lin Z, Pestell RG, Howell A, Aquila S, Andò S, Martinez-Outschoorn U, Sotgia F, Lisanti MP. Metabolic reprogramming of cancer-associated fibroblasts by TGF-β drives tumor growth: connecting TGF-β signaling with "Warburg-like" cancer metabolism and L-lactate production. Cell Cycle 2012; 11: 3019-3035.
[19] Yu JS, Cui W. Proliferation, survival and metabolism: the role of PI3K/AKT/mTOR signalling in pluripotency and cell fate determination. Development 2016; 143: 3050-3060.
[20] Hsiao CC, Keysselt K, Chen HY, Sittig D, Hamann J, Lin HH, Aust G. The adhesion GPCR CD97/ADGRE5 inhibits apoptosis. Int J Biochem Cell Biol 2015; 65: 197-208.
[21] Park SJ, Lee KP, Kang S, Chung HY, Bae YS, Okajima F, Im DS. Lysophosphatidylethanolamine utilizes LPA(1) and CD97 in MDA-MB-231 breast cancer cells. Cell Signal 2013; 25: 2147-2154.
[22] Ward Y, Lake R, Yin JJ, Heger CD, Raffeld M, Goldsmith PK, Merino M, Kelly K. LPA-receptor heterodimaerizes with CD97 to amplify LPA-initiated Rho-dependent signaling and invasion in prostate cancer cells. Cancer Res 2011; 71: 7301-7311.
[23] Wang X, Xiong Y, Zhang C, Zhou J, Yang J, Wang K, Xia X. Experimental study on inhibition of the growth of human adenoid cystic cancer cells by RNA interference targeting against survivin gene. Am J Transl Res 2016; 8: 375-383.
[24] Holliday DL, Speirs V. Choosing the right cell line for breast cancer research. Breast Cancer Res 2011; 13: 215.
[25] Hsiao HH, Cheng KF, Chen HY, Chou YH, Stacey M, Chang GW, Lin HH. Site-specific N-glycosylation regulates the GPS auto-proteolysis of CD97. FEBS Lett 2009; 583: 3285-3290.